RESEARCH ARTICLE

Tyrosine kinase inhibitor, masitinib, limits neuronal damage, as measured by serum neurofilament light chain concentration in a model of neuroimmune-driven neurodegenerative disease

Olivier Hermine[1,2]*, Laurent Gros[3], Truong-An Tran[3], Lamya Loussaief[3], Kathleen Flosseau[3], Alain Moussy[3], Colin D. Mansfield[3], Patrick Vermersch[4]

1 Imagine Institute, INSERM UMR 1163, University of Paris, Laboratory of Cellular and Molecular Mechanisms of Hematological Disorders and Therapeutic Implication, Hôpital Necker, Paris, France, **2** Department of Hematology, Necker Hospital, Assistance Publique Hôpitaux de Paris, Paris, France, **3** AB Science, Paris, France, **4** Univ. Lille, UMR Inserm U1172, CHU Lille, FHU Precise, Lille, France

* ohermine@gmail.com

Check for updates

OPEN ACCESS

Citation: Hermine O, Gros L, Tran T-A, Loussaief L, Flosseau K, Moussy A, et al. (2025) Tyrosine kinase inhibitor, masitinib, limits neuronal damage, as measured by serum neurofilament light chain concentration in a model of neuroimmune-driven neurodegenerative disease. PLoS One 20(5): e0322199. https://doi.org/10.1371/journal.pone.0322199

Editor: Masanori A. Murayama, Kansai Medical University: Kansai Ika Daigaku, Institute of Biomedical Science, JAPAN

Received: June 24, 2024

Accepted: March 17, 2025

Published: May 14, 2025

Copyright: © 2025 Hermine et al. This is an open access article distributed under the terms of the Creative Commons Attribution License, which permits unrestricted use, distribution, and reproduction in any medium, provided the original author and source are credited.

Data availability statement: All relevant data are within the manuscript and its Supporting information file.

Abstract

Background

Masitinib is an orally administered tyrosine kinase inhibitor that targets activated cells of the innate neuroimmune system. We have studied the neuroprotective action of masitinib on the manifestations of experimental autoimmune encephalitis (EAE) induced axonal and neuronal damage. EAE is a model of neuroimmune-driven chronic neuroinflammation and therefore highly relevant to masitinib's mechanism of action in neurodegenerative diseases. Importantly, neuronal damage, or prevention thereof, can be rapidly assessed by measuring serum neurofilament light chain (NfL) concentration in EAE-induced mice.

Methods

EAE induction was performed in healthy female C57BL/6 mice via active MOG 35–55 peptide immunization. Treatments were initiated 14 days post EAE induction. On day-0, 39 mice with established EAE symptoms were randomly assigned to 3 treatment groups (n = 13): EAE control, masitinib 50 mg/kg/day (M50), and masitinib 100 mg/kg/day (M100). The treatment started on day-1 and ended on day-15. Blood samples were collected on day-1 and day-8, via tail vein sampling, and on day-15, via intracardiac puncture. Assessments included quantification of serum NfL levels along the disease duration, cytokine quantification at day-15, and clinical assessments.

Funding: Masitinib is under clinical development by the study funder, AB Science, Paris, France. The funder participated in the design, conduct, management and reporting of the study. The funder collected and analyzed the data in conjunction with the authors, who contributed to manuscript draft revisions, provided critical comment, and approved submission for publication.

Competing interests: I have read the journal's policy and the authors of this manuscript have the following competing interests: Masitinib is under clinical development by the study funder, AB Science. AM, CDM, KF, LG, LL, OH, and TAT are employees and/or shareholders of AB Science. PV reports honoraria and consulting fees from Biogen, Sanofi-Genzyme, Novartis, Teva, Merck, Roche, Celgene, Imcyse and AB Science; and research grants from Sanofi-Genzyme, Roche and Merck.

Abbreviations: AD, Alzheimer's disease; ADAS-cog, Alzheimer's disease assessment scale-cognitive subscale; ALS, amyotrophic lateral sclerosis; ALSFRS-R, revised amyotrophic lateral sclerosis functional rating scale; CI, confidence intervals; Ctrl, EAE control group; CNS, central nervous system; CSF, cerebrospinal fluid; EAE, experimental autoimmune encephalitis; EDSS, expanded disability status scale; IFNg, interferon gamma; IL-1B, human interleukin-1 beta; IL-33, interleukin-33; KC/GRO, keratinocyte chemoattractant/human growth-regulated oncogene; M50, masitinib 50 mg/kg/day treatment group; M100, masitinib 100 mg/kg/day treatment group; MIP-2, macrophage inflammatory protein-2; MMSE, mini–mental state examination; MOG, myelin oligodendrocyte glycoprotein; MRI, magnet resonance imaging; MS, multiple sclerosis; N/A, not applicable; NDD, neurodegenerative disease; NfL, neurofilament light chain; SD, standard deviation; SEM, standard error of the mean; TNFa, tumor necrosis factor alpha.

Results

Masitinib treatment significantly ($p < 0.0001$) limited NfL production with respect to control; specifically, relative change in serum NfL concentration at day-8 was 43% and 60% lower for the M50 and M100 groups, respectively. Likewise, for the assessment of absolute serum NfL at day-8 and day-15, there was a significantly lower NfL concentration for masitinib treatment as compared with control. Furthermore, EAE mice treated with masitinib showed significantly lower concentrations of several well-established pro-inflammatory cytokines relative to control at day-15. A beneficial effect of masitinib on functional performance was also observed, with both M50 and M100 groups showing significantly less relative deterioration in grip strength at day-15 as compared with control ($p < 0.001$).

Conclusion

This study is the first demonstration that masitinib, a drug that targets the innate as opposed to the adaptive neuroimmune system, can lower serum NfL levels, and by extension therefore, neuronal damage, in a neuroimmune-driven neurodegenerative disease model. Overall, findings indicate that masitinib has a neuroprotective effect under conditions of chronic neuroinflammation and therefore plausible disease-modifying activity across a broad range of neurodegenerative diseases.

Background

The measurement of neurofilament light chain (NfL) in biological fluids has been proposed for monitoring the therapeutic effect of drugs aimed at reducing axonal damage. NfL are cytoskeletal proteins that are highly specific for neurons in both the central nervous system (CNS) and the peripheral nervous system. NfL in cerebrospinal fluid (CSF) or the bloodstream is therefore indicative of axonal lesions and/or degeneration and elevated NfL levels are associated with traumatic brain injuries or neurodegenerative diseases (NDD), including amyotrophic lateral sclerosis (ALS), multiple sclerosis (MS), and Alzheimer's disease (AD). Although this non-specificity limits the use of NfL as a diagnostic biomarker, a growing body of literature shows that because the level of free NfL in serum directly reflects neuronal damage within the CNS, it can be used as a reliable and easily accessible marker of disease intensity and/or activity across a variety of neurological disorders. As such, serum NfL is being widely touted as a future biomarker for prognosis, progression, and early detection of general neurodegenerative processes, as well as for monitoring the response of disease-modifying treatment [1,2].

In MS, clinical relapses and new/active MRI lesions (i.e., CNS injury caused by focal inflammation) result in the release of NfL. Thus, elevated levels of NfL are seen in the CSF and serum of patients with active MS and clinically isolated syndrome. In short-term prognosis studies, baseline serum NfL levels have been associated with worsening of the expanded disability status scale (EDSS) in the first year, number of

relapses, and progression of brain atrophy, while in long-term prognosis studies, both baseline and longitudinal measures of NfL levels have been linked to greater cerebral MRI-based brain atrophy [1,3]. The potential role of NfL as a promising long-term disability prognostic marker has also been demonstrated, with baseline serum NfL levels identified as the most efficient marker for distinguishing aggressive RRMS (defined as patients with an EDSS score of ≥6 at ≤15 years of follow-up) from benign RRMS (defined as patients with an EDSS score of ≤3 at ≥10 years of follow-up) [3]. Finally, serum NfL has been shown to significantly decrease in patients with active forms of MS following 12 months of treatment with disease-modifying therapies that target immune-mediated CNS injury, providing proof-of-concept for NfL as a marker of response to therapy in NDDs [1].

A growing body of scientific evidence supports the use of NfL as a prognostic biomarker in the broad ALS population, and a risk/susceptibility biomarker among a subset of SOD1 pathogenic variant carriers [4]. Notably, it has been shown that the baseline level of NfL in blood and CSF correlates with the speed and severity of ALS progression, with levels remaining relatively stable over time and disease stage [5–7]. Hence, serum NfL may one day provide a more objective and reliable pharmacodynamic biomarker for therapeutic trials than methods currently used for patient stratification and enrichment; e.g., the ALSFRS-R progression rate (ΔFS).

In patients with AD and mild cognitive impairment (MCI), there is a correlation between plasma NfL concentration and cognitive impairment, MRI hippocampal volume loss and brain atrophy. Moreover, higher plasma NfL levels predict faster cognitive deterioration and a higher rate of brain atrophy and hypometabolism in MCI patients over time [2]. The potential predictive biomarker utility of serum NfL was also demonstrated in familial Alzheimer's disease, with NfL dynamics predicting disease progression and brain neurodegeneration at the early presymptomatic stage of the disease [8].

Evidently therefore, NfL may become an indispensable biomarker for MS, ALS and AD to assess neuronal alterations. Indeed, regulatory proof of potential for this biomarker has now been established through the FDA approval of tofersen for ALS, based on that drug's ability to lower blood levels of NfL [9,10]. Importantly, NfL can serve as a biomarker of a drug's ability to produce a neuroprotective effect across a broad range of NDD indications, and any meaningful claim of clinical benefit is expected to be supported by a response in NfL.

Masitinib is a tyrosine kinase inhibitor that selectively inhibits c-Kit, colony-stimulating factor 1 receptor (CSF1R), LYN, and FYN, in the sub-micromolar range, and which is capable of accumulating in the CNS at therapeutically relevant concentrations [11,12]. Masitinib also inhibits cellular events mediated by activation of these receptor kinases, with its neuroprotective action resulting predominately from dual targeting of mast cell and microglia/macrophage activity and subsequent remodeling of the neuronal microenvironment. Microglia, macrophages and to a lesser extent mast cells, are types of innate immune cells that are present in the CNS and peripheral nervous system, and which are increasingly recognized as being involved in the pathophysiology of NDDs [13–26].

To date, masitinib has demonstrated neuroprotective benefits in three challenging NDDs; namely, mild-to-moderate AD, progressive forms of MS, and ALS, both in terms of preclinical models and clinical phase 2b/3 studies [27–37]. However, none of these studies performed fluid-based biomarker analysis. As such, evidence to support modification of underlying disease processes, and in particular neuroprotection resulting in the reduction of neuronal damage, is lacking. As an initial step to address this gap in our knowledge, we have studied the neuroprotective action of masitinib treatment on the manifestations of experimental autoimmune encephalitis (EAE) induced axonal and neuronal damage, using the MOG 35–55 peptide-induced EAE model. EAE is a CNS model of the neuroimmune system (including components of the innate immune system such as mast cells and microglia) that mimics aspects of MS and more generally the features of chronic neuroinflammation, which is a common pathological characteristic of most NDDs [38,39]. In EAE-affected mice, persistent axonal damage occurs from the early disease phase, as revealed by analysis of NfL leakage into the bloodstream along the disease duration, with clinical symptoms typically seen 12–16 days after disease induction (depending on EAE induction protocol and age of mice). Hence, axonal and neuronal damage, or prevention thereof, can be rapidly assessed by measuring serum NfL concentration in EAE-induced mice, along the disease duration.

Materials and methods

EAE model and negative (non EAE) control animals

A total of 60 female C57BL/6 mice, aged 9–11 weeks old, were purchased from the Charles River Laboratories (Saint-Germain-Nuelles, France). All mice were housed in individually ventilated cages of standard dimensions (maximum occupancy of 6 animals) in an environmentally monitored area (temperature and relative humidity), with sterilized litter, standard food and water *ad libitum*, at room temperature under a 14:10-hour light-dark cycle. Animals were acclimated to the study conditions for a period of 7 days prior to experimentation. Animals following the EAE protocol received diet supplementation (Dietgel® Recovery capsules) with their food pellets. No special procedure was followed for negative (non EAE) control mice.

Animals were monitored daily by authorized, qualified research staff and the following humane endpoints were used to determine when animals should be euthanized: general comportment (behavior) alteration, clinical score of greater than 3 (see section below on clinical assessments for details), or body weight loss of at least 20% at any time compared to baseline weight. Any animal reaching the humane endpoint was euthanized (via cervical dislocation) within 2 hours and all surviving animals were euthanized at the end of the study period (a total of 28 days post EAE induction).

Ethics approval

All experiments were performed in accordance with the European Directive 2010/63/EU and under valid experimental authorization issued by the French Research Ministry: APAFIS #45222-2023102009547945 v2. This experimental procedure was approved by the French experimental animal ethics committee n°051 (CERFE, approval D91228107) under the number 2023-011-B.

EAE model induction

EAE induction was performed in 47 healthy female mice (aged 10–12 weeks old) via active immunization using an EAE induction kit by Hooke Lab (MOG 35-55/CFA emulsion PTX, ref. EK-2110), administered subcutaneously at two sites (i.e., on midline of upper and lower back) at 0.1 ml/site (i.e., a total of 0.2 ml per mouse). Ready-to-use antigen (MOG 35-55) emulsion was kept on ice during the entire induction period. Immediately prior to injection, the pertussis toxin solution (PTX) was prepared by diluting the stock solution in cold PBS (2–8°C) to obtain a final concentration of 110 ng/µl. The solution was gently mixed by inverting (i.e., no vortexing) and kept on ice until used. The PTX solution was administered intraperitoneally at 0.1 mL/dose, 2 hours after antigen emulsion administration. This PTX procedure was repeated 24 hours later. The remaining 13 healthy mice were assigned to a negative (non EAE-induced) control group, in order to verify that EAE-induced treatment groups had successfully developed an EAE phenotype and were showing the expected axonal damage (as indicated by elevated serum NfL concentrations, and concomitant deterioration in clinical performance with disease progression). The quality of EAE induction was further verified via measurement of serum interleukin-17 (IL-17) concentration at D15, elevated levels of IL-17 being an established biomarker for development of EAE [40,41].

Experimental groups and blood sampling

Treatments were initiated 14 days post EAE induction. On Day 0 (D0), 39 mice with established EAE symptoms were randomly assigned to 3 treatment groups, comprising 13 mice per group (namely, EAE [vehicle] control, masitinib at 50 mg/kg/d, and masitinib at 100 mg/kg/d). Stratification of these EAE-induced mice was performed based on baseline rotarod performance, this parameter providing an earlier and more objective indication of EAE onset than clinical signs alone, thereby ensuring homogenous clinical functionality across groups at baseline. Treatment started on D1 and ended on D15. The test items, masitinib (AB Science, France) or its vehicle (NaCl 0.9%), were dosed twice a day (i.e., at 25 mg/kg or 50 mg/kg for the total daily doses of 50 mg/kg/d or 100 mg/kg/d) for 14 consecutive days by oral gavage applicator

with at least 6.5 hours between the 2 daily doses. Blood samples were collected from all animals once a week during the treatment period, at D1, D8 and D15. For intermediate blood sampling (D1 and D8 after the morning dose), up to 40 µl of whole blood was collected from each animal via tail vein sampling. Because samples drawn in this manner were too small for testing of individual animals it was necessary to pool these intermediate samples according to treatment group, the pooled sample being stored overnight at +4°C prior to serum separation via centrifugation at 5000 rpm for 10 minutes at +4°C. For terminal blood sampling on D15, intracardiac puncture was performed under general anesthesia with a solution of ketamine at 100 mg/kg (Ketamine®) and xylazine at 10 mg/kg (Rompun® 2%). At least 500 µl of whole blood was collected from each animal, thereby allowing for testing of individual animals, and stored for at least 2 hours at +4°C prior to serum separation via centrifugation at 1500 rpm for 20 minutes at +4°C. Serum samples were stored at −80°C until analysis.

Serum biomarker assessments

NfL levels in serum samples from EAE mice and negative controls were quantitated using the R-PLEX Human Neurofilament L assay (Catalog # K1517XR-2, Meso Scale Discovery), which employs advanced Meso Scale Discovery® (MSD) electrochemiluminescence (ECL)-based detection technology. Pooled serum samples from D1 and D8 were diluted 2-fold, 4-fold and 8-fold, and were run in duplicates (i.e., a total of 6 wells per sample). Likewise, pooled samples from D15 were diluted 4-fold, 8-fold and 16-fold, and run in duplicates (i.e., a total of 6 wells per sample). Individual sera from D15 were diluted 10-fold. The volume of original sample used was 25 µL of serum per replicate for the NfL quantification and 50 µL of serum per replicate for the cytokine quantification. Because of the larger sample volumes required for cytokine detection, this evaluation was conducted only for D15 intracardiac samples. Cytokines were quantified in serum samples using MSD's V-PLEX mouse cytokine panel 1 (K15245D) and V-PLEX Proinflammatory Panel 1 Mouse Kit (K15048D-1), according to the manufacture's instruction, for IFN-gamma, IL-1beta, IL-6, KC/GRO, IL-10, IL-12p70, IL-2, TNF-alpha, IL-33, IL-17A/F, MIP-2. The kit supplied calibrators were used as standards, calibration curves being constructed using 8 calibrators with concentrations ranging from 0 to 50,000 pg/mL for NfL and from 0 to 27,900 pg/mL for cytokines (depending on the cytokine tested). Analysis was done in the MSD Discovery Workbench software, with signals from calibrators fit to standard curves, which were then used for calculation of NfL and cytokine concentration in the samples.

Clinical assessments

The body weight of each animal was recorded twice per week. Each animal was observed twice a day over the study duration with any change in behavior, physical appearance or clinical signs recorded. Health status and disease progression were evaluated daily using an EAE-specific clinical scoring method, with scores and clinical observations related as follows: score of 0 – no obvious changes in motor function compared to non-immunized mice; 0.5 – tip of tail is limp; 1.0 – no signs of tail movement observed; 1.5 – limp tail and hind leg inhibition; 2.0 – limp tail and weakness of hind legs or poor balance; 2.5 – limp tail and dragging of hind legs; 3.0 – limp tail and complete paralysis of hind legs; 3.5 – limp tail and complete paralysis of hind legs in addition to no righting reflex (euthanasia recommended); 4.0 – limp tail, complete hind leg, and partial front leg paralysis (euthanasia recommended); 4.5 – complete hind and partial front leg paralysis with no movement around the cage (euthanasia recommended); 5.0 – dead or mouse is spontaneously rolling in the cage (euthanasia recommended).

The effect of masitinib on motor coordination and muscle tone was evaluated by the rotarod test and grip strength test, with animals tested under non-blind conditions. Disease progression impairs motor coordination/muscle tone, thereby decreasing the time (seconds) an animal can remain on a rotating rod or decreasing the grip force (forelimb and hindlimb) recorded via a strain gauge in Newtons (N). Both tests were performed twice a week, in the morning, at least 1 hour after starting the light circadian cycle. Mice were evaluated on the rotating rod with a starting speed of four rotations per

minute (rpm) and acceleration up to the maximum speed of 40 rpm within 300 s (i.e., a single acceleration ramp of 1 rpm every 8.3 s). Each mouse was tested in 3 consecutive trials, with 2–5 minutes between trials, and the best score retained for analysis. Grip strength was obtained by pulling the animal backwards along the platform until the animal's paws grab the mesh grip piece on the push-pull gauge. The animal was gently pulled backwards with consistent force by the experimenter until it released its grip. Again, each mouse was tested in 3 consecutive trials and the best score was retained for analysis.

Data analysis

Relative change in NfL over time was calculated at D8 relative to D1, using pooled tail vein samples according to treatment group. Because D15 blood samples were collected via intracardiac puncture, intergroup comparison was based on absolute NfL and cytokines concentrations at this single, terminal timepoint. Analysis of pooled samples was performed on replica tests (2 duplicates of 3 dilutions per sample). All group values are presented as mean and standard error of the mean (SEM), with statistical comparisons computed using the unpaired t-test. All statistical analyses were performed with GraphPad Prism10. Statistical significance is indicated by an asterisk * for $p \leq 0.05$, ** for $p \leq 0.01$, *** for $p \leq 0.001$, **** for $p \leq 0.0001$.

Results

Baseline characteristics and EAE disease course

Table 1 shows that at the time of treatment initiation (D1, 14 days post EAE induction), the EAE treatment groups showed a clear deterioration of functional performance (as measured by rotarod test, grip strength and clinical score) and deterioration of axonal integrity (as measured by serum NfL concentration), when compared with the negative (non-EAE) control group. These observations are consistent with the description of the EAE model.

Comparison of absolute NfL measurements at D1 served as a check of possible bias in axonal damage at baseline. Clinical baseline characteristics were balanced between the masitinib treatment arms, but both arms appeared to show slightly more severe disease relative to the EAE control group, as evidenced by the latter having a lower NfL concentration (7.3 versus 9.4 and 13.5 ng/ml), higher function scores (grip strength 198 versus 172 and 183 N; rotarod 109 versus 100 and 100 s), and lower clinical score (0.35 versus 0.58 and 0.58). One mouse from the EAE control group was euthanized at D8, according to the ethical criteria. All the other animals were alive and with a clinical score of less than 3.5 at the terminal timepoint (D15).

All clinical assessments, including average relative changes in grip strength, clinical score, rotarod performance, and body weight, showed a significant ($p < 0.001$) worsening during the treatment period (D1 to D15) for the EAE control group with respect to the non-EAE cohort (which conversely remained stable). Such deterioration in clinical performance is consistent with the description of the EAE model. The quality of EAE induction was further verified via measurement of

Table 1. Baseline characteristics at time of treatment initiation (D1) according to treatment group.

Experimental group	n	Rotarod (s)	Body weight (g)	Grip strength (N)	Clinical score	Serum NfL (ng/ml)	D1 Relative NfL*
Negative [non-EAE] control	13	167.1 ± 15.3	19.8 ± 0.3	229.4 ± 8.4	0	3.2 ± 0.04	N/A
EAE [vehicle] control	13	109.4 ± 17.2	19.5 ± 0.6	197.9 ± 16.1	0.35 ± 0.13	7.3 ± 0.2	1.0
Masitinib 50 mg/kg/d	13	100.4 ± 13.5	19.2 ± 0.5	172.3 ± 14.8	0.58 ± 0.12	9.4 ± 0.2	1.3
Masitinib 100 mg/kg/d	13	100.2 ± 12.4	19.4 ± 0.3	183.1 ± 13.0	0.58 ± 0.10	13.5 ± 0.2	1.8

Values are expressed as mean ± SEM.

*D1 Relative NfL is the ratio of concentrations with respect to the EAE [vehicle] control group.

N/A = not applicable.

https://doi.org/10.1371/journal.pone.0322199.t001

serum interleukin-17 (IL-17) concentration at D15, with each EAE-induced treatment group showing an approximate 2-fold increase relative to the negative (non-EAE) control group.

Masitinib slows deterioration of grip strength in the EAE mouse model

The non-EAE cohort served as a negative control group to verify that EAE-induced animals were experiencing a deterioration in clinical performance consistent with the description of the EAE model. All clinical assessments, including average relative changes in grip strength, clinical score, rotarod performance, and body weight, showed a significant ($p < 0.001$) worsening during the treatment period (D1 to D15) for the EAE control group with respect to the non-EAE cohort (which conversely remained stable), confirming development of an EAE phenotype. A beneficial effect of masitinib on functional performance was observed in terms of grip strength. While there was a significant deterioration in relative grip strength over the 15-day treatment period for the EAE control group as compared with the negative control group, the grip strength capabilities of masitinib treated mice initially deteriorated but then recovered to their pretreatment (D1) level by D15. Indeed, both the 50 and 100 mg/kg/d masitinib groups showed significantly less relative deterioration in grip strength at D15 with respect to the EAE control group ($p < 0.001$) (Fig 1). Conversely, there was no discernable difference between EAE control and masitinib treated groups for any of the other clinical assessments over the treatment period.

Masitinib reduces serum NfL concentration in the EAE mouse model

As expected, all EAE groups showed an increased concentration of serum NfL with disease evolution, while that of the negative control group remained stable or decreased slightly. However, assessment of relative change in serum NfL concentration over a duration of 8 days (pooled tail vein sampling) showed that masitinib treatment significantly reduced NfL production in EAE mice with respect to the EAE control group (Fig 2A and Table 2). The relative increase at D8 with

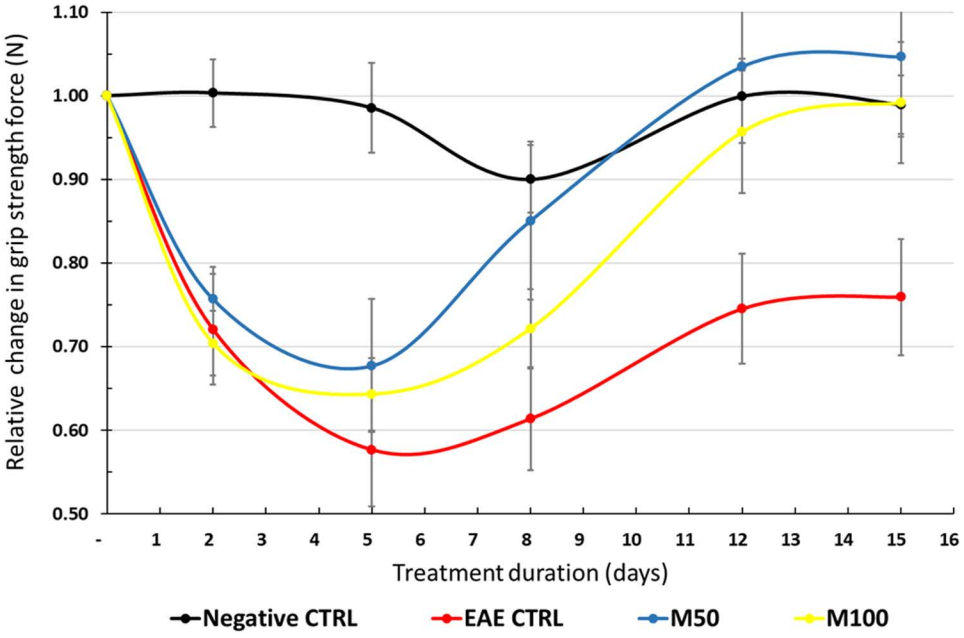

Fig 1. Average relative deterioration in grip strength force (N) over treatment period, according to treatment group. CTRL = EAE control group. M50 = Masitinib 50 mg/kg/d. M100 = Masitinib 100 mg/kg/d. N = Newtons. Relative grip strength normalized to value at start of treatment period (D0). Values are expressed as mean ± SEM.

https://doi.org/10.1371/journal.pone.0322199.g001

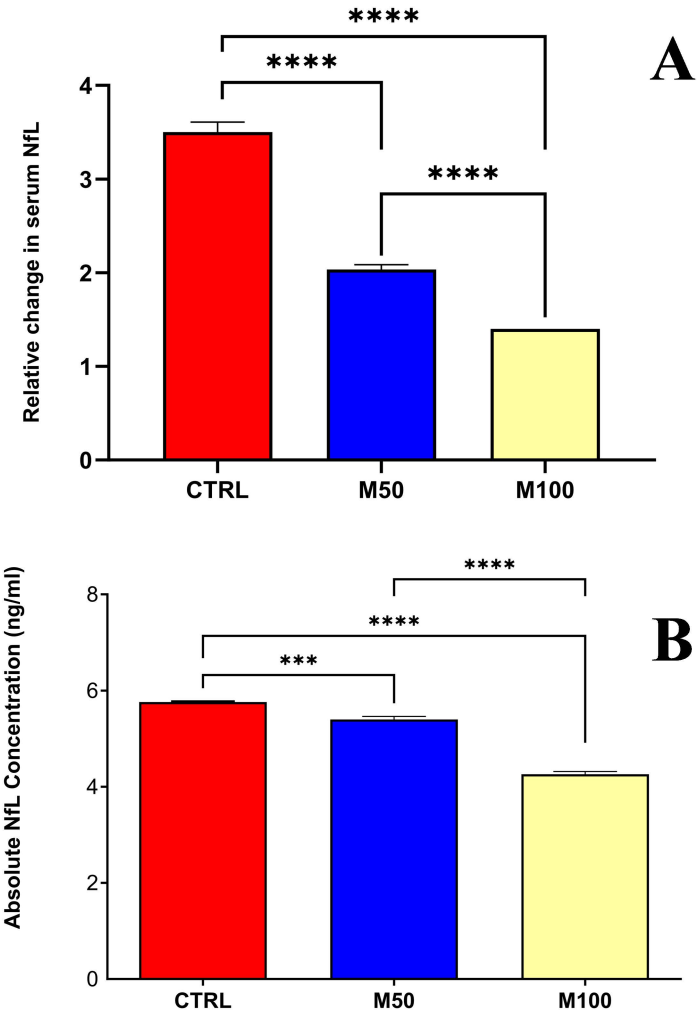

Fig 2. (A) Day-8 relative change from baseline in serum NfL concentrations, according to treatment group. (B) Day-15 absolute serum NfL concentrations, according to treatment group. CTRL = EAE control group. M50 = Masitinib 50 mg/kg/d. M100 = Masitinib 100 mg/kg/d. Values are expressed as mean ± SEM. Statistical significance (unpaired t-test) is indicated by an asterisk * p < 0.05, *** for p < 0.001, **** for p < 0.0001.

https://doi.org/10.1371/journal.pone.0322199.g002

Table 2. Assessment of serum NfL concentration – Relative change in serum NfL concentration over time (D8 relative to D1), and D8 absolute concentration.

Experimental group	n	Absolute NfL at D1 (ng/ml)	Absolute NfL at D8 (ng/ml)	Relative Change (D8:D1)	(D8:D1) Relative difference in NfL	p-value†	D8 Relative Difference in NfL absolute concentration	p-value†
EAE [vehicle] control	13	7.3 ± 0.21	25.7 ± 0.67	3.5	N/A	N/A	N/A	N/A
Masitinib 50 mg/kg/d	13	9.4 ± 0.21	19.2 ± 0.39	2	−43%	< 0.0001	−25%	< 0.05
Masitinib 100 mg/kg/d	13	13.5 ± 0.24	18.8 ± 0.44	1.4	−60%	< 0.0001	−27%	< 0.05

Values are expressed as mean ± SEM. P-value with respect to the EAE [vehicle] control group.

†Unpaired t-test with respect to the EAE [vehicle] control group.

*D8 Relative Difference NfL is the proportional difference in concentrations with respect to the EAE [vehicle] control group.

N/A = not applicable.

https://doi.org/10.1371/journal.pone.0322199.t002

respect to D1 was 3.5-fold for the EAE control group, which was a significantly greater relative change than either the 50 mg/kg/d masitinib group (2-fold increase at D8 with respect to D1, $p < 0.0001$), or the 100 mg/kg/d masitinib group (1.4-fold increase at D8 with respect to D1, $p < 0.0001$). This corresponds to a reduction in serum NfL concentration, relative to the EAE control group, of 43% and 60% for the masitinib 50 mg/kg/d and masitinib 100 mg/kg/d groups, respectively (Table 2). Pairwise comparison of the masitinib groups also showed a dose-dependent effect with a significantly smaller relative change for masitinib 100 mg/kg/d as compared with masitinib 50 mg/kg/d ($p < 0.0001$) (Fig 2A).

Consistent with what was seen for the relative change in serum NfL over 8 days, the absolute concentration at D8 was significantly lower by approximately 25% for both masitinib treatment groups (50 and 100 mg/kg/d) relative to the EAE control group ($p < 0.0001$) (Table 2). By comparison, at baseline (D1) the EAE control group NfL concentration had started at a lower absolute concentration than both masitinib groups (Table 1).

Likewise, for the assessment of serum NfL at D15, there was a significantly lower concentration for both masitinib treatment groups (50 and 100 mg/kg/d) as compared with the EAE control group (Fig 2B). The treatment effect was more pronounced for the masitinib 100 mg/kg/d group as compared with the masitinib 50 mg/kg/d group, with an average lower concentration than the EAE control group of 26% ($p < 0.0001$) and 6% ($p < 0.001$), respectively, and a significant dose-dependency ($p < 0.0001$) between masitinib groups. Due to the larger quantity of serum collected from intracardiac puncture sampling, it was possible to also assess samples from each individual animal. As seen in Fig 3, there is a large inter-subject spread of NfL concentrations, however, the average values generally reflect the pooled D15 results, with a significantly lower concentration for the masitinib 100 mg/kg/d treatment group relative to the EAE control group ($p < 0.0037$), and a significant dose-dependency ($p < 0.0086$) between masitinib groups.

Masitinib decreases pro-inflammatory cytokine biomarker concentrations in the EAE mouse model

Cytokines that are important in inflammatory responses and immune system regulation, including those associated with Th1/Th2 pathway biomarkers, were quantified to determine whether masitinib treatment was associated with lower levels of these inflammatory biomarkers. Serum samples from D15, collected using the intracardiac puncture procedure, were used for this analysis because of the larger volume requirements necessary.

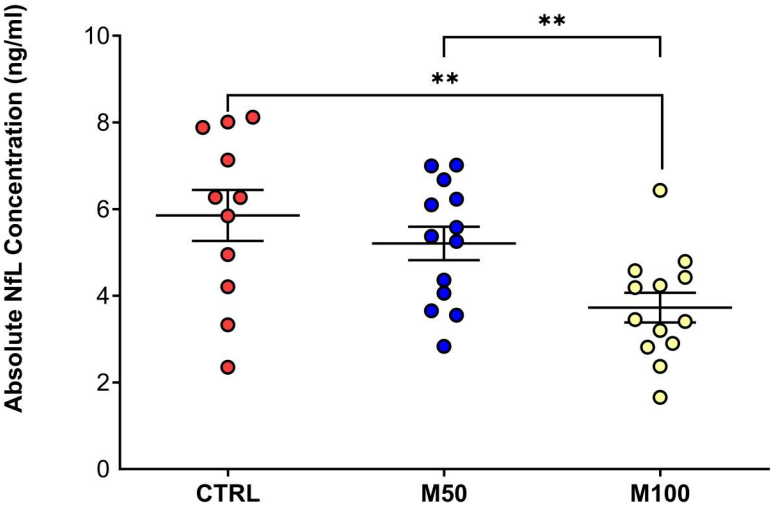

Fig 3. Day-15 absolute serum NfL concentrations from individual animals, according to treatment group. CTRL = EAE control group. M50 = Masitinib 50 mg/kg/d. M100 = Masitinib 100 mg/kg/d. Values are expressed as mean ± SEM. Statistical significance (unpaired t-test) is indicated by an asterisk * $p < 0.05$, ** for $p < 0.01$.

https://doi.org/10.1371/journal.pone.0322199.g003

Overall, EAE mice treated with masitinib showed significantly lower concentrations of several well-established pro-inflammatory cytokines, i.e., interferon gamma, tumor necrosis factor alpha, human interleukin-1 beta, interleukin-33, KC/GRO, MIP-2, as compared with the EAE control group (Table 3). This is consistent with a reduction in neuroinflammatory activity.

Interferon gamma (IFNg), also known as immune interferon, is a pro-inflammatory cytokine produced by lymphocytes and is a potent activator of macrophages. It plays physiologically important roles in promoting innate and adaptive immune responses, and is involved in the regulation of anti-inflammatory responses. The absolute concentration of IFNg at D15 was significantly lower for the masitinib 50 mg/kg/d and masitinib 100 mg/kg/d groups relative to the EAE control group, by 40% and 34%, respectively (i.e., 1.8 ± 0.6 and 2.1 ± 0.1 versus 3.1 ± 0.2 pg/ml, respectively).

Tumor necrosis factor alpha (TNFa) is an inflammatory cytokine that is mainly secreted by macrophages. The absolute concentration of TNFa at D15 was significantly lower for the masitinib 50 mg/kg/d and masitinib 100 mg/kg/d groups relative to the EAE control group, by 22% and 10%, respectively (i.e., 13.4 ± 0.9 and 15.4 ± 0.2 versus 17.1 ± 0.1 pg/ml, respectively).

Human interleukin-1 beta (IL-1b) is a pro-inflammatory cytokine that is produced by macrophages/monocytes during acute inflammation, and which contributes to a variety of NDDs. The absolute concentration of IL-1b at D15 was significantly lower for the masitinib 50 mg/kg/d and masitinib 100 mg/kg/d groups relative to the EAE control group, by 33% and 37%, respectively (i.e., 0.7 ± 0.2 and 0.6 ± 0.1 versus 1.0 ± 0.1 pg/ml, respectively).

Interleukin-33 (IL-33) is a member of the IL-1 cytokine family and is crucial for induction of Th2-type cytokine-associated immune responses. Its expression is upregulated following pro-inflammatory stimulation. The absolute concentration of IL-33 at D15 was significantly lower for the masitinib 50 mg/kg/d and masitinib 100 mg/kg/d groups relative to the EAE control group, by 82% and 48%, respectively (i.e., 0.8 ± 0.2 and 2.4 ± 0.8 versus 4.7 ± 0.2 pg/ml, respectively).

Keratinocyte chemoattractant (KC)/human growth-regulated oncogene (GRO) (KC/GRO) is a CXC chemokine that is involved in neutrophil activation and recruitment during inflammation. The absolute concentration of KC/GRO at D15 was significantly lower for the masitinib 100 mg/kg/d group, relative to the EAE control group by 15% (i.e., 50.7 ± 3.8 versus 59.6 ± 1.5 pg/ml, respectively).

Table 3. Relative difference in serum cytokine concentrations with respect to the EAE control group following 15 days of treatment.

	n	IFNg			TNFa			IL-1b		
		Conc (pg/µL)	Rel Diff (%)	p	Conc (pg/µL)	Rel Diff (%)	p	Conc (pg/µL)	Rel Diff (%)	p
Ctrl	11	3.11	N/A		17.13	N/A		1.01	N/A	
M50	13	1.85	−40 ± 18	< 0.0001	13.37	−22 ± 5	< 0.0001	0.68	−33 ± 15	< 0.0092
M100	13	2.05	−34 ± 1	< 0.0001	15.36	−10 ± 1	< 0.0036	0.64	−37 ± 5	< 0.0011
	n	KC/GRO			IL-33			MIP-2		
		Conc (pg/µL)	Rel Diff (%)	p	Conc (pg/µL)	Rel Diff (%)	p	Conc (pg/µL)	Rel Diff (%)	p
Ctrl	11	5.96	N/A		4.73	N/A		11.98	N/A	
M50	13	60.53	+2 ± 3	ns	0.85	−82 ± 4	< 0.0001	11.52	−4 ± 3	ns
M100	13	50.66	−15 ± 4	< 0.0004	2.44	−48 ± 14	< 0.0001	9.47	−21 ± 10	< 0.0004

M50 = Masitinib 50 mg/kg/d. M100 = Masitinib 100 mg/kg/d. Ctrl = EAE control group. Values are expressed as mean ± SEM. ns = statistically non-significant. P = p-value calculated via unpaired t-test. N/A = not applicable. IFNg = Interferon gamma. TNFa = Tumor necrosis factor alpha. IL-1B = Human interleukin-1 beta. KC/GRO = Keratinocyte chemoattractant/human growth-regulated oncogene. IL-33 = Interleukin-33. MIP-2 = Macrophage inflammatory protein-2.

https://doi.org/10.1371/journal.pone.0322199.t003

Macrophage inflammatory protein (MIP-2) is a CXC chemokine, also known as chemokine CXC ligand (CXCL2), that affects neutrophil recruitment and activation. The absolute concentration of MIP-2 at D15 was significantly lower for the masitinib 100 mg/kg/d group relative to the EAE control group by 21% (i.e., 9.5 ± 1.6 versus 12.0 ± 0.6 pg/ml, respectively).

Other tested cytokines, i.e., IL-6, IL-17, IL-2, IL-10 and IL-12p70, showed no discernable difference between EAE control and masitinib treated groups.

Discussion

This study is the first demonstration that masitinib can lower serum NfL levels in a neuroimmune-driven neurodegenerative disease model, with concomitant reduction in pro-inflammatory cytokines and slowing of clinical (EAE) symptoms. Strengths of this study are that it used the well-established MOG 35–55 peptide-induced EAE model of neuroimmune-driven chronic neuroinflammation, which is highly relevant to masitinib's mechanism of action (i.e., targeting of the innate neuroimmune system and in particular mast cells and microglia). Because chronic neuroinflammation is a common pathological characteristic of most NDDs, these results should have broad applicability across a range of indications. Moreover, data was derived after disease onset (i.e., in a therapeutic setting as opposed to an asymptomatic preventative setting), which is of greater relevance because such models more closely simulate the clinical condition of NDD patients and therefore better represent their therapeutic needs.

The main limitation of this study was insufficient sample volume to perform both NfL and cytokine assays at multiple timepoints across the study duration. This constraint comes from the animals' general state of health, which is profoundly weakened by EAE, with a consequence that the volume of blood available varies according to the animal's state of health. To avoid any sample collection bias, we therefore took the same, minimum (tail vein) volume from each animal for the longitudinal analysis of relative change in NfL and the larger (intracardiac) volume required for cytokine analysis only at the synchronized endpoint. The use of dissimilar blood collection techniques at different timepoints (i.e., tail vein at D1 and D8 versus intracardiac at D15), precluded calculation of relative NfL change after D8. It would therefore be useful to confirm these findings over a longer treatment period and in a larger sample size, using a sample collection schedule that permits longitudinal analysis of relative NfL change over multiple timepoints and with tail vein collection just prior to the intracardiac collection. Finally, the synchronized 14-day endpoint was prespecified to facilitate biomarker analysis, however, this relatively short treatment duration may not have allowed for measurable cytokine changes (i.e., due to therapeutic lag), with a consequence that the effects of masitinib may be underestimated. Ideally, any confirmatory findings would also be supported by pathological data showing a correlation between neuronal preservation and NfL concentration, as well as assessment of mast cell activation markers to better discriminate the respective contributions of microglia and mast cells.

Remarkably, masitinib has so far demonstrated clinical benefit in three challenging neurodegenerative disorders with an acceptable safety profile given the high unmet medical need of these indications [27–29,42]. In progressive forms of MS, masitinib administered at 4.5 mg/kg/d showed a statistically significant reduction in cumulative change on EDSS score ($p = 0.0256$) [28]. This treatment-effect was consistent for both primary progressive MS and non-active secondary progressive patient subgroups. Masitinib also significantly reduced the risk of reaching an EDSS score of 7.0, corresponding to disability severe enough that the patient is restricted to a wheelchair ($p = 0.0093$). The rationale to use masitinib in progressive forms of MS is supported by evidence from the literature, showing that progressive MS is driven by activity of the innate immune system, compartmentalized within the CNS [15,19,23,43–46].

In mild-to-moderate AD, masitinib administered at 4.5 mg/kg/d as an add-on therapy to standard of care, significantly slowed cognitive deterioration relative to placebo with a manageable safety profile. More specifically, the between-group difference in the Alzheimer's disease assessment scale-cognitive subscale (ADAS-cog) change from baseline at week 24 was −2.15 (97.5%CI [−3.48, −0.81]), $p = 0.0003$ [27]. This change is considered clinically

meaningful, especially when considering its administration on a background of cholinesterase inhibitors and memantine, a 2-point change being consistent with published recommendations [47] and benchmark ADAS-Cog benefit according to well-established therapies [48–50]. The rationale to use masitinib in AD is supported by preclinical evidence demonstrating that the pharmacological action of masitinib in mast cells can restore normal spatial learning performance in a mouse model of AD and promotes recovery of synaptic markers [13,36]. Overall, these findings are consistent with a growing body of evidence implicating mast cells and microglia with the pathophysiology of AD [21–26,51–56].

In ALS, masitinib administered at 4.5 mg/kg/d as an add-on to standard riluzole, significantly slowed functional decline at week 48 relative to riluzole alone by 27% [29]. For the prespecified primary efficacy population, there was a between-group difference in ALSFRS-R change from baseline of 3.4 points (95%CI [0.65; 6.13]; p = 0.016). Moreover, long-term follow-up analysis showed a significantly prolonged survival of 25 months (p = 0.0478) and 44% reduced risk of death (hazard ratio 0.56 (95%CI [0.32;0 .96]), Cox p = 0.036), if treatment was initiated at an early stage of disease [30]. Masitinib's mechanism of action in ALS has been well-demonstrated in the preclinical setting, with data showing that masitinib co-targets independent pathological mechanisms in different cell types of the brain, spinal cord and peripheral nervous system components that taken together conserves neuro-muscular function [12,31–35]. Again, these findings are consistent with accumulating evidence indicating that immune dysfunction and neuroinflammation are important pathological characteristics of ALS [23,24,57–60].

Hence, the preclinical biomarker data reported here, taken together with the positive clinical outcomes and growing body of literature described above, support a proposition that modulation of the neuroimmune system via inhibition of microglia and/or mast cell activity, is a valid therapeutic strategy across a broad range of NDD indications. Individually, each of these neuroimmune cells represents a viable target for therapeutic intervention, with the dual-targeting of masitinib making it a particularly attractive treatment option.

Conclusions

These results provide further evidence regarding the anti neuro-inflammatory properties of masitinib. Importantly, the observed NfL treatment response supports the assertion that masitinib has a neuroprotective effect under conditions of chronic neuroinflammation and therefore plausible disease-modifying activity in each of the NDDs for which it has shown clinical benefit, i.e. progressive forms of MS, ALS, and mild-to-moderate AD.

Supporting information

S1 Appendix. Dataset.
(PDF)

Author contributions

Conceptualization: Olivier Hermine, Laurent Gros, Truong-An Tran, Lamya Loussaief, Kathleen Flosseau, Alain Moussy, Patrick Vermersch.

Data curation: Laurent Gros, Truong-An Tran, Lamya Loussaief, Kathleen Flosseau.

Formal analysis: Laurent Gros, Truong-An Tran, Lamya Loussaief, Colin D. Mansfield.

Supervision: Alain Moussy.

Writing – original draft: Colin D. Mansfield.

Writing – review & editing: Olivier Hermine, Laurent Gros, Truong-An Tran, Lamya Loussaief, Kathleen Flosseau, Alain Moussy, Colin D. Mansfield, Patrick Vermersch.

References

1. Gaetani L, Blennow K, Calabresi P, Di Filippo M, Parnetti L, Zetterberg H. Neurofilament light chain as a biomarker in neurological disorders. J Neurol Neurosurg Psychiatry. 2019;90(8):870–881. https://doi.org/10.1136/jnnp-2018-320106 PMID: 30967444
2. Palermo G, Mazzucchi S, Della Vecchia A, Siciliano G, Bonuccelli U, Azuar C, et al. Different clinical contexts of use of blood neurofilament light chain protein in the spectrum of neurodegenerative diseases. Mol Neurobiol. 2020;57(11):4667–91. https://doi.org/10.1007/s12035-020-02035-9 PMID: 32772223
3. Arroyo Pereiro P, Muñoz-Vendrell A, León Moreno I, Bau L, Matas E, Romero-Pinel L, et al. Baseline serum neurofilament light chain levels differentiate aggressive from benign forms of relapsing-remitting multiple sclerosis: a 20-year follow-up cohort. J Neurol. 2024;271(4):1599–609. https://doi.org/10.1007/s00415-023-12135-w PMID: 38085343
4. Benatar M, Ostrow LW, Lewcock JW, Bennett F, Shefner J, Bowser R, et al. Biomarker qualification for neurofilament light chain in amyotrophic lateral sclerosis: theory and practice. Ann Neurol. 2024;95(2):211–216. https://doi.org/10.1002/ana.26860 PMID: 38110839
5. Verde F, Otto M, Silani V. Neurofilament light chain as biomarker for amyotrophic lateral sclerosis and frontotemporal dementia. Front Neurosci. 2021;15:679199. https://doi.org/10.3389/fnins.2021.679199 PMID: 34234641
6. Bjornevik K, O'Reilly EJ, Molsberry S. Neurofilament light chain levels in amyotrophic lateral sclerosis. Neurology. 2021;97(15):e1466–74.
7. Witzel S, Statland JM, Steinacker P, Otto M, Dorst J, Schuster J, et al. Longitudinal course of neurofilament light chain levels in amyotrophic lateral sclerosis-insights from a completed randomized controlled trial with rasagiline. Eur J Neurol. 2024;31(3):e16154. https://doi.org/10.1111/ene.16154 PMID: 37975796
8. Preische O, Schultz SA, Apel A, Kuhle J, Kaeser SA, Barro C, et al. Serum neurofilament dynamics predicts neurodegeneration and clinical progression in presymptomatic Alzheimer's disease. Nat Med. 2019;25(2):277–283. https://doi.org/10.1038/s41591-018-0304-3 PMID: 30664784
9. FDA 2023. Press release 04/25/2023 FDA approves treatment of amyotrophic lateral sclerosis associated with a mutation in the SOD1 gene. [cited 19 Dec 2023]. Available from: https://www.fda.gov/drugs/news-events-human-drugs/fda-approves-treatment-amyotrophic-lateral-sclerosis-associated-mutation-sod1-gene
10. Meyer T, Schumann P, Weydt P, Petri S, Koc Y, Spittel S, et al. Neurofilament light-chain response during therapy with antisense oligonucleotide tofersen in SOD1-related ALS: treatment experience in clinical practice. Muscle Nerve. 2023;67(6):515–521. https://doi.org/10.1002/mus.27818 PMID: 36928619
11. Dubreuil P, Letard S, Ciufolini M, Gros L, Humbert M, Castéran N, et al. Masitinib (AB1010), a potent and selective tyrosine kinase inhibitor targeting KIT. PLoS One. 2009;4(9):e7258. https://doi.org/10.1371/journal.pone.0007258 PMID: 19789626
12. Trias E, Ibarburu S, Barreto-Núñez R, Babdor J, Maciel TT, Guillo M, et al. Post-paralysis tyrosine kinase inhibition with masitinib abrogates neuroinflammation and slows disease progression in inherited amyotrophic lateral sclerosis. J Neuroinflammation. 2016;13(1):177. https://doi.org/10.1186/s12974-016-0620-9 PMID: 27400786
13. Lin CJ, Herisson F, Le H, Jaafar N, Chetal K, Oram MK, et al. Mast cell deficiency improves cognition and enhances disease-associated microglia in 5XFAD mice. Cell Rep. 2023;42(9):113141. https://doi.org/10.1016/j.celrep.2023.113141 PMID: 37713312
14. Mado H, Adamczyk-Sowa M, Sowa P. Role of microglial cells in the pathophysiology of MS: synergistic or antagonistic? Int J Mol Sci. 2023;24(3):1861. https://doi.org/10.3390/ijms24031861 PMID: 36768183
15. Kamma E, Lasisi W, Libner C, Ng HS, Plemel JR. Central nervous system macrophages in progressive multiple sclerosis: relationship to neurodegeneration and therapeutics. J Neuroinflammation. 2022;19(1):45. https://doi.org/10.1186/s12974-022-02408-y PMID: 35144628
16. Sandhu JK, Kulka M. Decoding mast cell-microglia communication in neurodegenerative diseases. Int J Mol Sci. 2021;22(3):1093. https://doi.org/10.3390/ijms22031093 PMID: 33499208
17. Muzio L, Viotti A, Martino G. Microglia in neuroinflammation and neurodegeneration: from understanding to therapy. Front Neurosci. 2021;15:742065.
18. Harcha PA, Garcés P, Arredondo C, Fernández G, Sáez JC, van Zundert B. Mast cell and astrocyte hemichannels and their role in Alzheimer's disease, ALS, and harmful stress conditions. Int J Mol Sci. 2021;22(4):1924. https://doi.org/10.3390/ijms22041924 PMID: 33672031
19. Pinke KH, Zorzella-Pezavento SFG, Lara VS, Sartori A. Should mast cells be considered therapeutic targets in multiple sclerosis? Neural Regen Res. 2020;15(11):1995–2007. https://doi.org/10.4103/1673-5374.282238 PMID: 32394947
20. Hagan N, Kane JL, Grover D. CSF1R signaling is a regulator of pathogenesis in progressive MS. Cell Death Dis. 2020;11(10):904. https://doi.org/10.1038/s41419-020-03084-7 PMID: 33097690
21. Schwabe T, Srinivasan K, Rhinn H. Shifting paradigms: the central role of microglia in Alzheimer's disease. Neurobiol Dis. 2020;143:104962. PMID: 32535152
22. Long JM, Holtzman DM. Alzheimer disease: an update on pathobiology and treatment strategies. Cell. 2019; 179(2):312–339.
23. Jones MK, Nair A, Gupta M. Mast Cells in Neurodegenerative Disease. Front Cell Neurosci. 2019;13:171. https://doi.org/10.3389/fncel.2019.00171 PMID: 31133804
24. Skaper SD, Facci L, Zusso M, Giusti P. An inflammation-centric view of neurological disease: beyond the neuron. Front Cell Neurosci. 2018;12:72. https://doi.org/10.3389/fncel.2018.00072 PMID: 29618972

25. Hendriksen E, van Bergeijk D, Oosting RS, Redegeld FA. Mast cells in neuroinflammation and brain disorders. Neurosci Biobehav Rev. 2017;79:119–133. https://doi.org/10.1016/j.neubiorev.2017.05.001 PMID: 28499503
26. Shaik-Dasthagirisaheb YB, Conti P. The role of mast cells in Alzheimer's disease. Adv Clin Exp Med. 2016;25(4):781–7. https://doi.org/10.17219/acem/61914 PMID: 27629855
27. Dubois B, López-Arrieta J, Lipschitz S, Doskas T, Spiru L, Moroz S, et al. Masitinib for mild-to-moderate Alzheimer's disease: results from a randomized, placebo-controlled, phase 3, clinical trial. Alzheimers Res Ther. 2023;15(1):39. https://doi.org/10.1186/s13195-023-01169-x PMID: 36849969
28. Vermersch P, Brieva-Ruiz L, Fox RJ, et al. Efficacy and safety of masitinib in progressive forms of multiple sclerosis: a randomized, phase 3, clinical trial. Neurol Neuroimmunol Neuroinflamm. 2022;9(3):e1148
29. Mora JS, Genge A, Chio A, Estol CJ, Chaverri D, Hernández M, et al. Masitinib as an add-on therapy to riluzole in patients with amyotrophic lateral sclerosis: a randomized clinical trial. Amyotroph Lateral Scler Frontotemporal Degener. 2020;21(1-2):5–14. https://doi.org/10.1080/21678421.2019.1632346 PMID: 31280619
30. Mora JS, Bradley WG, Chaverri D, Hernández-Barral M, Mascias J, Gamez J, et al. Long-term survival analysis of masitinib in amyotrophic lateral sclerosis. Ther Adv Neurol Disord. 2021;14:17562864211030365. https://doi.org/10.1177/17562864211030365 PMID: 34457038
31. Kovacs M, Alamón C, Maciel C, Varela V, Ibarburu S, Tarragó L, et al. The pathogenic role of c-Kit+ mast cells in the spinal motor neuron-vascular niche in ALS. Acta Neuropathol Commun. 2021;9(1):136. https://doi.org/10.1186/s40478-021-01241-3 PMID: 34389060
32. Trias E, Kovacs M, King PH. Schwann cells orchestrate peripheral nerve inflammation through the expression of CSF1, IL-34, and SCF in amyotrophic lateral sclerosis. Glia. 2020;68(6):1165-1181.
33. Harrison JM, Rafuse VF. Muscle fiber-type specific terminal Schwann cell pathology leads to sprouting deficits following partial denervation in SOD1G93A mice. Neurobiol Dis. 2020;145:105052. https://doi.org/10.1016/j.nbd.2020.105052 PMID: 32827689
34. Trias E, King PH, Si Y, Kwon Y, Varela V, Ibarburu S, et al. Mast cells and neutrophils mediate peripheral motor pathway degeneration in ALS. JCI Insight. 2018;3(19):e123249. https://doi.org/10.1172/jci.insight.123249 PMID: 30282815
35. Trias E, Ibarburu S, Barreto-Núñez R, Varela V, Moura IC, Dubreuil P, et al. Evidence for mast cells contributing to neuromuscular pathology in an inherited model of ALS. JCI Insight. 2017;2(20):e95934. https://doi.org/10.1172/jci.insight.95934 PMID: 29046475
36. Li T, Martin E, Abada Y-S, Boucher C, Cès A, Youssef I, et al. Effects of chronic masitinib treatment in APPswe/PSEN1dE9 transgenic mice modeling Alzheimer's disease. J Alzheimers Dis. 2020;76(4):1339–1345. https://doi.org/10.3233/JAD-200466 PMID: 32623401
37. Vermersch P, Benrabah R, Schmidt N, Zéphir H, Clavelou P, Vongsouthi C, et al. Masitinib treatment in patients with progressive multiple sclerosis: a randomized pilot study. BMC Neurol. 2012;12:36. https://doi.org/10.1186/1471-2377-12-36 PMID: 22691628
38. Zhang W, Xiao D, Mao Q, Xia H. Role of neuroinflammation in neurodegeneration development. Signal Transduct Target Ther. 2023;8(1):267. https://doi.org/10.1038/s41392-023-01486-5 PMID: 37433768
39. Kwon HS, Koh SH. Neuroinflammation in neurodegenerative disorders: the roles of microglia and astrocytes. Transl Neurodegener. 2020;9(1):42.
40. Murayama MA, Chi H-H, Matsuoka M, Ono T, Iwakura Y. The CTRP3-AdipoR2 axis regulates the development of experimental autoimmune encephalomyelitis by suppressing Th17 cell differentiation. Front Immunol. 2021;12:607346. https://doi.org/10.3389/fimmu.2021.607346 PMID: 34925309
41. Komiyama Y, Nakae S, Matsuki T, Nambu A, Ishigame H, Kakuta S, et al. IL-17 plays an important role in the development of experimental autoimmune encephalomyelitis. J Immunol. 2006;177(1):566–573. https://doi.org/10.4049/jimmunol.177.1.566 PMID: 16785554
42. Hamad AA, Amer BE. Safety of masitinib in patients with neurodegenerative diseases: a meta-analysis of randomized controlled trials. Neurol Sci. 2024;45(7):3503–7. https://doi.org/10.1007/s10072-024-07502-y PMID: 38627298
43. Mahmood A, Miron VE. Microglia as therapeutic targets for central nervous system remyelination. Curr Opin Pharmacol. 2022;63:102188. https://doi.org/10.1016/j.coph.2022.102188 PMID: 35219055
44. Stys PK, Tsutsui S. Recent advances in understanding multiple sclerosis. F1000Res. 2019;8:F1000 Faculty Rev-2100.
45. Brown MA, Tanzola MB, Robbie-Ryan M. Mechanisms underlying mast cell influence on EAE disease course. Mol Immunol. 2002;38(16–18):1373–8. https://doi.org/10.1016/s0161-5890(02)00091-3 PMID: 12217411
46. Luo C, Jian C, Liao Y. The role of microglia in multiple sclerosis. Neuropsychiatr Dis Treat. 2017;13:1661–1667.
47. Vellas B, Andrieu S, Sampaio C, Coley N, Wilcock G, European Task Force Group. Endpoints for trials in Alzheimer's disease: a European task force consensus. Lancet Neurol. 2008;7(5):436–450. https://doi.org/10.1016/S1474-4422(08)70087-5 PMID: 18420157
48. Birks JS, Harvey RJ. Donepezil for dementia due to Alzheimer's disease. Cochrane Database Syst Rev. 2018;6(6):CD001190. https://doi.org/10.1002/14651858.CD001190.pub3 PMID: 29923184
49. Birks JS, Chong LY, Grimley Evans J. Rivastigmine for Alzheimer's disease. Cochrane Database Syst Rev. 2015;9(9):CD001191. https://doi.org/10.1002/14651858.CD001191.pub4 PMID: 26393402
50. Birks J. Cholinesterase inhibitors for Alzheimer's disease. Cochrane Database Syst Rev. 2006;2006(1):CD005593. https://doi.org/10.1002/14651858.CD005593 PMID: 16437532

51. Leng F, Edison P. Neuroinflammation and microglial activation in Alzheimer disease: where do we go from here? Nat Rev Neurol. 2021;17(3):157–172.
52. Kang YJ, Diep YN, Tran M, Cho H. Therapeutic targeting strategies for early- to late-staged Alzheimer's disease. Int J Mol Sci. 2020;21(24):9591. https://doi.org/10.3390/ijms21249591 PMID: 33339351
53. Nordengen K, Kirsebom B-E, Henjum K, Selnes P, Gísladóttir B, Wettergreen M, et al. Glial activation and inflammation along the Alzheimer's disease continuum. J Neuroinflammation. 2019;16(1):46. https://doi.org/10.1186/s12974-019-1399-2 PMID: 30791945
54. Fani Maleki A, Rivest S. Innate immune cells: monocytes, monocyte-derived macrophages and microglia as therapeutic targets for Alzheimer's disease and multiple sclerosis. Front Cell Neurosci. 2019;13:355.
55. Kempuraj D, Mentor S, Thangavel R, Ahmed ME, Selvakumar GP, Raikwar SP, et al. Mast cells in stress, pain, blood-brain barrier, neuroinflammation and Alzheimer's disease. Front Cell Neurosci. 2019;13:54. https://doi.org/10.3389/fncel.2019.00054 PMID: 30837843
56. Hansen DV, Hanson JE, Sheng M. Microglia in Alzheimer's disease. J Cell Biol. 2018;217(2):459–472. https://doi.org/10.1083/jcb.201709069 PMID: 29196460
57. Vahsen BF, Gray E, Thompson AG, Ansorge O, Anthony DC, Cowley SA, et al. Non-neuronal cells in amyotrophic lateral sclerosis - from pathogenesis to biomarkers. Nat Rev Neurol. 2021;17(6):333–348. https://doi.org/10.1038/s41582-021-00487-8 PMID: 33927394
58. Clarke BE, Patani R. The microglial component of amyotrophic lateral sclerosis. Brain. 2020;143(12):3526–39. https://doi.org/10.1093/brain/awaa309 PMID: 33427296
59. Iyer AK, Jones KJ, Sanders VM, Walker CL. Temporospatial analysis and new players in the immunology of amyotrophic lateral sclerosis. Int J Mol Sci. 2018;19(2):631. https://doi.org/10.3390/ijms19020631 PMID: 29473876
60. Crisafulli SG, Brajkovic S, Cipolat Mis MS, Parente V, Corti S. Therapeutic strategies under development targeting inflammatory mechanisms in amyotrophic lateral sclerosis. Mol Neurobiol. 2018;55(4):2789–2813. https://doi.org/10.1007/s12035-017-0532-4 PMID: 28455693